Clin Orthop Relat Res (2013) 471:2808–2814
DOI 10.1007/s11999-013-2867-0

Clinical Orthopaedics and Related Research®
A Publication of The Association of Bone and Joint Surgeons®

SYMPOSIUM: TSCHERNE FESTSCHRIFT

Implant Material and Design Alter Construct Stiffness in Distal Femur Locking Plate Fixation: A Pilot Study

Ulf Schmidt MD, Rainer Penzkofer PhD, Samuel Bachmaier MSc, Peter Augat PhD

Published online: 23 February 2013

Abstract

Background Construct stiffness affects healing of bones fixed with locking plates. However, variable construct stiffness reported in the literature may be attributable to differing test configurations and direct comparisons may clarify these differences.

Questions/purposes We therefore asked whether different distal femur locking plate systems and constructs will lead to different (1) axial and rotational stiffness and (2) fatigue under cyclic loading.

Methods We investigated four plate systems for distal femur fixation (AxSOS, LCP, PERI-LOC, POLYAX) of differing designs and materials using bone substitutes in a distal femur fracture model (OTA/AO 33-A3). We created six constructs of each of the four plating systems. Stiffness under static and cyclic loading and fatigue under cyclic loading were measured.

Results Mean construct stiffness under axial loading was highest for AxSOS (100.8 N/mm) followed by PERI-LOC (80.8 N/mm) and LCP (62.6 N/mm). POLYAX construct stiffness testing showed the lowest stiffness (51.7 N/mm) with 50% stiffness of AxSOS construct testing. Mean construct stiffness under torsional loading was similar in the group of AxSOS and PERI-LOC (3.40 Nm/degree versus 3.15 Nm/degree) and in the group of LCP and POLYAX (2.63 Nm/degree versus 2.56 Nm/degree). The fourth load level of $> 75{,}000$ cycles was reached by three of six AxSOS, three of six POLYAX, and two of six PERI-LOC constructs. All others including all LCP constructs failed earlier.

Conclusions Implant design and material of new-generation distal femur locking plate systems leads to a wide range of differences in construct stiffness.

The institution of one of the authors (US) has received, during the study period, funding from the Association for Orthopaedic Research (AFOR) and from the Osteosynthesis and Trauma Care Foundation. The institution of one of the authors (PA) has received funding from Stryker Osteosynthesis (Stryker GmbH, Selzach, Switzerland), Smith & Nephew Inc (Memphis, TN, USA), Aesculap (Tuttlingen, Germany), Arthrex (Munich, Germany), and Synthes (Bettlach, Switzerland). One of the authors (SB) is an employee of Arthrex.
All ICMJE Conflict of Interest Forms for authors and *Clinical Orthopaedics and Related Research* editors and board members are on file with the publication and can be viewed on request. *Clinical Orthopaedics and Related Research* neither advocates nor endorses the use of any treatment, drug, or device. Readers are encouraged to always seek additional information, including FDA-approval status, of any drug or device prior to clinical use.
This work was performed at the Institute of Biomechanics, Trauma Center Murnau, Murnau, Germany, and at the Department of Material Science, Regensburg University of Applied Sciences, Regensburg, Germany.

U. Schmidt (✉)
Department of Trauma Orthopaedic Surgery,
Krankenhaus der Barmherzigen Schwestern Ried,
Schlossberg 1, 4910 Ried im Innkreis, Austria
e-mail: ulf.schmidt@bhs.at

R. Penzkofer, P. Augat
Institute of Biomechanics, Trauma Center Murnau,
Murnau, Germany

S. Bachmaier
Department of Material Science, Regensburg University
of Applied Sciences, Regensburg, Germany

P. Augat
Institute of Biomechanics, Paracelsus Medical University
Salzburg, Salzburg, Austria

Clinical Relevance Assuming construct stiffness affects fracture healing, these data may influence surgical decision-making in choosing an implant system.

Introduction

As a result of the aging population, the incidence of fractures of the distal femur is increasing [19], especially in patients with osteoporosis. During the past decade, retrograde intramedullary devices [20] as well as new generations of distal femur locked plating systems [9] have facilitated the operative treatment of these fractures. Clinically, locked plating systems are an established alternative to intramedullary nails [9, 12, 22]. However, 0% to 23% of patients will experience healing complications such as delayed union, hardware failures, and/or nonunion [10, 13].

Biomechanical [4] and clinical studies [10] suggest that mechanical factors such as implant and construct stiffness are a potential cause of difficulties in fracture healing in periarticular femur fractures. Henderson et al. [10] suggested stainless steel locking plates are associated with a higher percentage of nonunions than titanium plates (57% versus 43%, respectively). Many investigators have explored comparisons of distal femur locked plating systems with intramedullary nail systems [19, 20, 25], angled blade plates [11, 24, 25], dynamic condylar screws [11], and locked plating constructs with different screw configurations in the condylar fragment of the fracture model [8, 16]. However, reported stiffness values for the same implant vary up to more than one order of magnitude, perhaps as a result of differing configurations of the bone-implant constructs (BICs) or test equipment. The current data, therefore, are difficult to interpret. Comparable data of the newest-generation distal femur locking plates requires direct comparisons in one test configuration.

We then asked whether different distal femur locking plate systems and constructs will lead to differing (1) axial and rotational stiffness and (2) fatigue under cyclic loading.

Materials and Methods

We compared four locked plating systems (Table 1) for fixing distal femur fractures in a biomechanical experiment. An extraarticular distal femur fracture type, AO/OTA 33-A3 [15], was simulated using artificial bone substitutes and a 25-mm defect zone (Fig. 1). Of each plating system, six BICs were nondestructively loaded in the axial direction and torsion to determine stiffness. Afterward each BIC was cyclically loaded with increasing load levels until failure.

To simulate a defect fracture, we prepared fiber-filled epoxy cylinders to model the cortical shell of the diaphysis with an outer diameter of 35 mm, a wall thickness of 4 mm, and a length of 250 mm. The condylar fragment was modeled by cancellous bone substitute material, Solid Rigid Polyurethane Foam (Sawbones, Malmö, Sweden), with dimensions of $90 \times 70 \times 55$ mm^3 and a density of 15 pcf (240 kg/m^3). Each defect fracture model was fixed with one of four plating systems (Table 1). All screws were inserted at the shaft area in a bicortical locking configuration (Fig. 2). In the condylar area, we inserted five unicortical fixed-angle locking screws according to the manufacturer's specifications in the AxSOS (Stryker, Selzach, Switzerland), LCP (Synthes, Bettlach, Switzerland), and PERI-LOC (Smith & Nephew, Memphis, TN, USA) constructs. In the POLYAX system (DePuy, Leeds, UK), five unicortical polyaxial screws were inserted in the condylar area perpendicular to the plate and in a parallel fashion comparable to the other plate systems. To estimate the elastic range and the level of failure load for subsequent stiffness measurements, pretests were made with two BICs (one for axial compression and one for torsion). From each implant system, six constructs were first nondestructively loaded within the elastic range and were then cyclically tested until failure. The necessary sample size of the study was determined a priori using the software SPSS Sample Power 2 (SPSS Inc, Chicago, IL, USA). We were unable to identify any literature to suggest what differences in construct stiffness might result in clinically important differences. Using six samples per group, this pilot study would be able to identify group differences of 1.5 SDs based on a confidence level of 95% and power of 80%.

The test apparatus was designed to apply axial eccentric compression load and torsional loads (Fig. 2) and was adapted from a test setup reported by Wähnert et al. [19] that allows cardanic joints. This configuration would simulate the axial and torsional loads experienced during ground-level walking [17, 18]. For axial compression testing, we fixed the BICs between two universal joints. The eccentric loading test configuration was adapted from Gaebler et al. [7] made suitable for distal femur testing [20]. The rotational degree of freedom (vertical axis) of the proximal universal joint was free and therefore eliminating torsional loads. For torsion testing, the BICs were fixed between a distal universal joint and a proximal linear bearing to eliminate transverse loads in the horizontal plane. All tests were performed on servohydraulic testing machines with 10 kN/100-Nm load cells (Instron 8874; Instron, Pfungstadt, Germany).

The overall deformation of the BIC in loading direction was measured using the internal device of the test machine measuring the grip-to-grip motion. To measure displacement directly at the fracture site, an optical deformation measurement system (GOM mbH, Braunschweig, Germany) calculated angular changes between the foam block

Table 1. Plate length and screws of the four locked plating systems

Group	POLYAX	LCP	AxSOS	PERI-LOC
Manufacturer	DePuy (Leeds, UK)	Synthes (Bettlach, Switzerland)	Stryker (Selzach, Switzerland)	Smith & Nephew (Memphis, TN, USA)
Material	Titanium alloy	Titanium alloy	Stainless steel	Stainless steel
Implant system	Distal femoral locked plate system 9-hole	Distal femur 9-hole	Distal lateral femur 10-hole	Distal femur locking plate 10-hole
	Locked cannulated screw FT, 8 × 65 mm	Locked screw 5 × 40 mm	Locked screw 5 × 40 mm + insert	Locked screw 4.5 × 40 mm
	Locked cortical screw FT, 4.5 mm × 4.5 mm	Locked screw 5 × 60 mm	Locked screw 5 × 60 mm	Locked screw 4.5 × 60 mm
	Polyaxial screw FT, 5.5 mm × 65 mm			

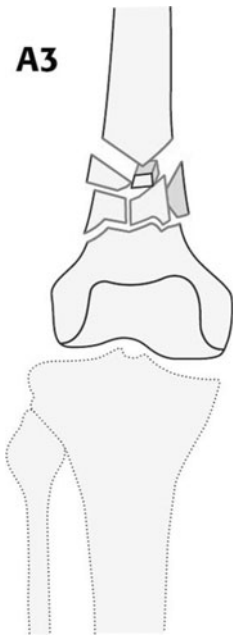

Fig. 1 Type AO/OTA A3-33 fracture of the distal femur is demonstrated with a supracondylar comminution zone.

(distal condyle) and epoxy tube (femoral shaft). The overall deformation measurement from the test machine correlated with ($r^2 = 0.90$) the optical deformation measurement.

One BIC of each group was tested to failure in a static axial and torque test with a plunger speed of 0.1 mm/s and 0.1°/s [20], respectively. Load and displacement were recorded at a frequency of 20 Hz for estimation of the yield loads. The yield loads were used to determine the linear elastic region at which the static stiffness tests were performed. Thus stiffness testing always was nondestructive and remained within the linear elastic region for each implant.

We performed nondestructive static testing on six BICs for axial and torsional loading. The tests in axial compression and torsion were performed to calculate the construct stiffness of the BIC from the slope of the load displacement curve. We applied three cycles of preconditioning up to a peak load of 60% of the linear elastic range of the BIC to obtain more stable readings and then recorded loading of all constructs twice. We applied loads in displacement control using a plunger speed of 0.2 mm/s (axial compression) followed by the torsion test with 0.15°/s (torsion). The loading regimen for loading used in our study is based on comparable testing methodologies used by other authors [14, 20] and is considered representative of physiologic postoperative loading of the distal femur based the results of in vivo telemetry studies [6, 17, 18].

Cyclic tests were only performed under axial loading using the six BICs from the nondestructive construct stiffness tests. We applied a cyclic sinusoidal load to each plate system in load control at 1.5 Hz from a preload level of 50% of the maximum load applied in the static tests. The different preload levels were implemented to achieve a number of load cycles until fatigue failure. According to the staircase method, the load level increases after every 25,000 cycles with a load increment of 10%. The minimum of load amplitude was defined by 70% of the corresponding load level. Data were recorded within each load level after 100, 5000, 10,000, 15,000, 20,000, and 25,000 load cycles. The failure of bone substitute or implant materials was defined as an end criterion. Also, failure of a BIC was defined when an angle $\alpha = 10°$ was reached (clinical failure criterion). This was determined with postprocess image analysis because the tests were stopped at an angle of 17° (technical limitation of the setup). No breakage of bone substitute cylinder tubes, screws, or plates occurred with one exception: screw loosening occurred once for a LCP construct. We documented the fracture pattern of each BIC with photography.

For all implant systems we calculated the load cycle integral. The load cycle integral is the area below the staircase starting at zero load cycles and ending at the load cycle where failure was detected. The load cycle integral is a measurement to compare the destructive energy until failure.

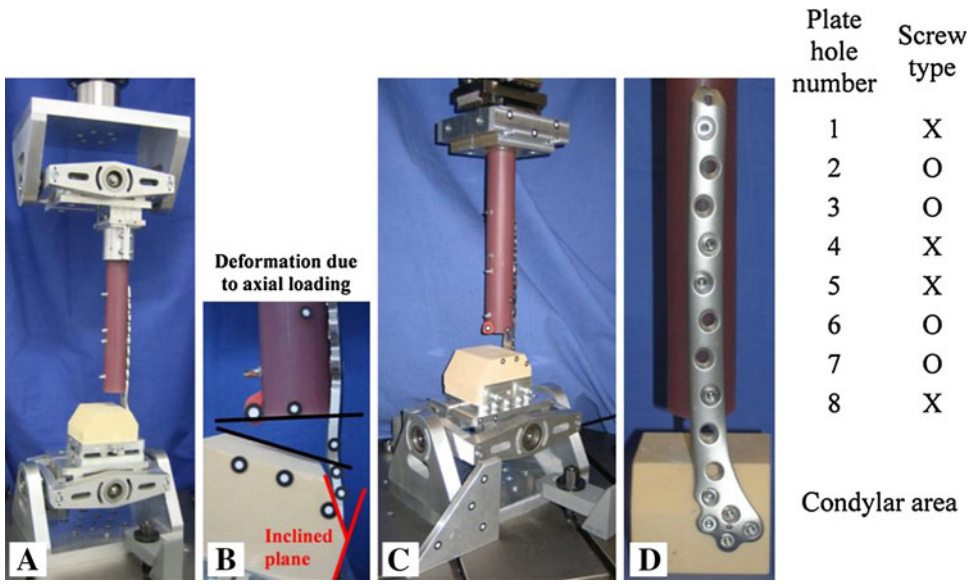

Fig. 2A–D (**A**) Test setup for eccentric axial loading using a cardanic joint distally and proximally. (**B**) Deformation of the construct resulting from axial loading. Note the inclined plane of 33° for anatomical fit of the plates. (**C**) Torsional loading was realized with a cardanic joint distally and two horizontal linear bearings proximally. (**D**) Example of the standardized screw configuration in the shaft area of the bone implant constructs with four bicortical screws: 1 = most proximal plate hole; X = bicortical locking screw; O = no screw/empty plate hole; 8 = distal.

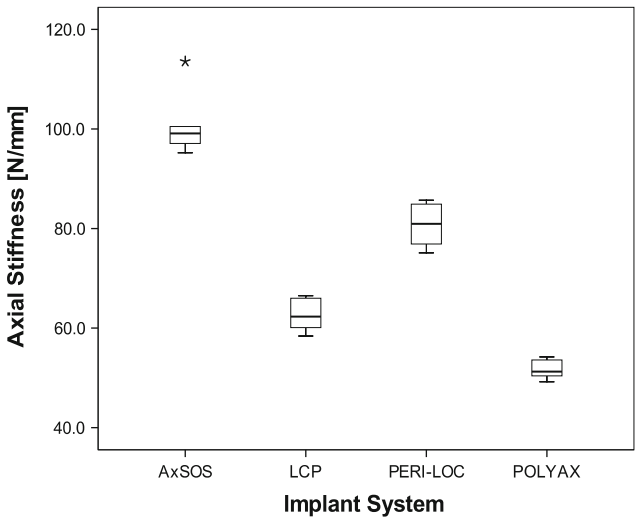

Fig. 3 Box-and-whisker plot of the axial construct stiffness (N/mm) under static loading. The box shows the interquartile range (IQR) and the whiskers extend to the smallest and largest values except data points with distance greater than 1.5 times IQR. The black line within the box represents the median. Outliers are data points lying between 1.5 times IQR and three times IQR. Extremes are data points beyond three times IQR and were marked as asterisks (*). All data points were included for statistical analysis. The highest stiffness was found for AxSOS followed by PERI-LOC, LCP, and POLYAX (n = 6 per implant system).

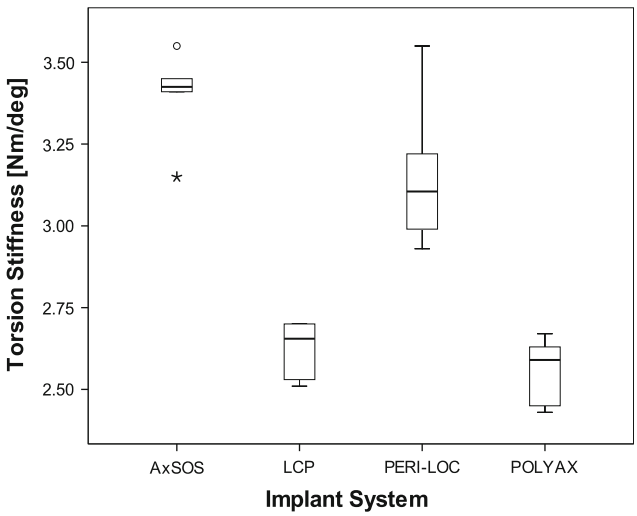

Fig. 4 Box-and-whisker plot of the torsional construct stiffness (Nm/degree) under static loading. The box shows the interquartile range (IQR) and the whiskers extend to the smallest and largest values except data points with distance greater than 1.5 times IQR. The black line within the box represents the median. Outliers are data points lying between 1.5 times IQR and three times IQR and were marked as circles (°). Extremes are data points beyond three times IQR and were marked as asterisks (*). All data points were included for statistical analysis. The highest stiffness was found for AxSOS followed by PERI-LOC, LCP, and POLYAX (n = 6 per implant system).

We compared stiffness under static loading and cyclic fatigue among the four groups using the Kruskal-Wallis test/exact test according to the Monte Carlo method; the Monte Carlo estimate of the p value was based on 10,000 samples with a 95% confidence level. In the case of major differences, we performed subsequent analyses between two independent groups of the test results using the two-tailed Mann-Whitney U test (including the Monte Carlo-exact test method). The analyses were run with the software PASW Statistics 17.0 (SPSS Inc).

Results

We found differences in mean axial and torsional stiffness between the implants made of steel versus the two implants

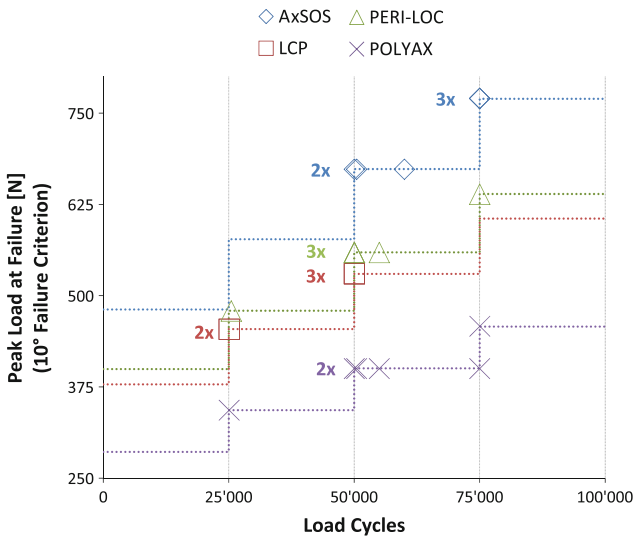

Fig. 5 The load cycle and peak load at the time of failure (10° displacement) are demonstrated for each BIC (n = 6 per implant system, n = 5 for LCP).

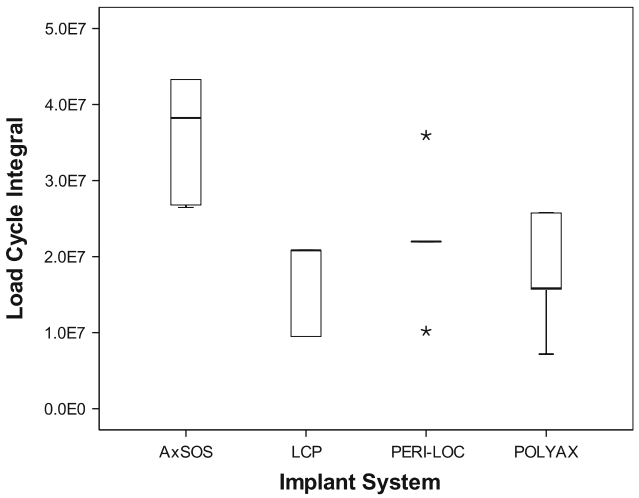

Fig. 6 Box-and-whisker plot of the load cycle integral of all implant systems. The box shows the interquartile range (IQR) and the whiskers extend to the smallest and largest values except data points with distance greater than 1.5 times IQR. The black line within the box represents the median. Outliers are data points lying between 1.5 times IQR and three times IQR. Extremes are data points beyond three times IQR and were marked as asterisks (*). All data points were included for statistical analysis. We found differences between all systems except for PERI-LOC and POLYAX and for LCP and POLYAX.

made of titanium. Axial stiffness of each of the two steel plates (AxSOS and PERI-LOC) was larger (p = 0.002) than for the two titanium plates (LCP and POLYAX). The differences in axial stiffness between implants of different material were as large as 95% (POLYAX versus AxSOS; p = 0.002). Among the two steel implants, the AxSOS plate provided 10% larger stiffness (p = 0.002) compared with the PERI-LOC, whereas the PERI-LOC construct was 30% stiffer (P = 0.002) compared with the LCP construct (Fig. 3). We observed comparable relative torsional stiffness between the constructs as for axial stiffness. Again both steel implants were stiffer (p = 0.003) by up to 32% than titanium implants. However, among the implants with the same material, torsional stiffness was similar (p > 0.07) (Fig. 4).

Under cyclic fatigue testing, one implant system made of steel (AxSOS) had higher survival compared with the other steel implant and the two titanium implants. All BICs failed by reaching the failure criterion of 10° angular displacement except one BIC of the LCP system, which failed by screw loosening. Most BICs failed at the beginning or during the third load level at 50,000 load cycles (Fig. 5). The analysis of the load cycle integral indicated that the AxSOS construct had higher survival compared with the two titanium implants (p = 0.005) but also compared with the PERI-LOC steel plate (p = 0.014). Although none of the LCP plates survived the first load cycles of the third load level, no differences in survival (p = 0.893) were observed between LCP and POLYAX titanium plates (Fig. 6).

Discussion

As a result of the improved fixation strength they provide, periarticular locking plates have become a standard of care in the treatment of distal femur fractures. Many of these fractures had uneventful but deficient healing as been reported and has also been associated with the mechanical performance of fracture fixation [3, 9]. The mechanical performance of fracture fixation differs considerably among different implant fixation systems [11, 19, 20, 24, 25] but state-of-the-art systems have so far not been compared using consistent assessment methodology. To perform a direct comparison with multiple new-generation distal femur locking plates, we biomechanically evaluated four plating systems addressing two questions: will different distal femur locking plate systems and constructs lead to differing (1) axial and rotational stiffness and (2) fatigue under cyclic loading?

Our study had some limitations. First, like with most biomechanical tests, the chosen loading configuration represents only a singular loading scenario. Although comparable load scenarios should yield comparable findings, different loading configurations such as pure bending or pure shear loading might yield different findings even relative differences between the constructs. We chose the loads that would be experienced during ground-level walking to be most relevant for the survival of the implant and most characteristic for loads experienced at the fracture site during daily activities. Second, the simplified test setup did also not simulate soft tissue forces and we did not

validate our synthetic bone model with human cadaveric bones. The test setup used in our study was adapted from the study of Wähnert et al. [20] who validated this test setup and protocol with human cadaveric bones. They found the test scenario to yield qualitatively similar results for cadaveric and synthetic bones with similar failure modes and only small differences in quantitative results. Soft tissue and muscles tend to stabilize a fracture. Thus, neglecting these forces represents a worst case scenario for the testing of BICs. Third, the tested implant systems differed in length of the shaft, monoaxial or polyaxial screw fixation, and screw diameter. Although these variations clearly affect the biomechanical properties of the plating system [23], they also represent the clinical reality of different implant designs. This influence of the variations was minimized by using the same working length as well as the same number and configuration of the screws in the shaft and in the condylar area. Changing one of the specifications (eg, increasing the distance between bone surface and plate) will certainly change the mechanical performance and although we assume the change to be similar for all the constructs tested, we cannot exclude that some specific changes in the specifications may distort our findings. Fourth, to evaluate our biomechanical study design, a comparison with studies with a similar setup, bone substitute material, and comparable implant systems is important. Studies fulfilling these criteria [3, 20, 23] report an axial construct stiffness within a range from 63 N/mm to 168 N/mm. Our results of axial stiffness of the tested implant systems lie within these ranges. Even more, the mean axial stiffness of the AxSOS plate systems tested in our study is similar to that of AxSOS plate systems (110 N/mm) reported by Wähnert et al. [20]. The loading regimen for axial loading used in our study is based on comparable testing methodologies used by other authors [14, 20]. The incremental axial loading applied in these studies is considered representative of physiologic postoperative loading of the distal femur and based the results of in vivo telemetry studies [6, 17, 18]. With our cyclic loading protocol of 25,000 cycles per load level, we tried to simulate increasing walking forces over a 2-month period. However, none of our BICs reached 100,000 cycles and/or forces of 1870 N, which is considered as a loading regimen simulating physiologic forces over a 2-month period [5]. Our fracture model represents an extraarticular fracture, which is classified as a type of distal femur fracture [15] associated with substantial complication rates [16]. This model is used in multiple biomechanical studies [5, 11, 14, 21, 25]. The fracture model used in our study with a fracture gap of 25 mm may not correlate with the clinical fracture pattern; however, it was created to perform a worst case fracture pattern without any inherent stability. Finally, biological factors that may affect the stiffness by using the same implant such as differences in size, weight, or bone density or individual healing response are not addressed by this study. The basic concept was to provide comparable data of bone implant constructs using one standardized test setup.

In our direct comparison of four different implant constructs, we found the two steel implants provided larger axial stiffness and to some extent also larger torsional stiffness compared with the two titanium implants. Fatigue strength of the implant constructs, however, appeared more strongly related to implant design than to implant material.

Axial and torsional stiffness determines the amount of movement at the fracture defect zone and may thus trigger the healing response of bone by providing the necessary mechanical signal for the stimulation of fracture healing [2]. Extreme values of stiffness could potentially jeopardize the healing response of bone by providing insufficient or excessive amounts of interfragmentary movement. Findings from our study may help to explain findings of delayed healing and inhibition of periosteal callus formation in distal femur fractures fixed with stainless steel plates [10]. Highest axial stiffness values were obtained with the AxSOS and the PERI-LOC constructs, both made of stainless steel. Axial stiffness values obtained by the two titanium implants were more than 30% smaller and may thus provide a different mechanical stimulus for fracture healing. Although axial micromotion at the fracture site is known to stimulate healing, torsional motion induces shear at the fracture site and may be more critical for successful fracture healing [1]. Torsional stiffness again was largest for the steel plate with the AxSOS design. Although Otto et al. [16] used a different test setup, under axial loading, they similarly showed LISS (LCP) had 25% greater stiffness than POLYAX. Torsional construct stiffness differed between the implant systems showing 19% to 31% higher values of the constructs with steel implant systems (AxSOS and PERI-LOC) versus constructs with titanium implants. Except the study of Otto et al. [16], no further comparisons of the implant systems that we tested were are available in the literature.

Cyclic axial fatigue testing with our study protocol showed superior durability for the AxSOS implant system with the highest load cycle integral. Studies with a comparable protocol for cyclic loading are missing. These results might suggest that the implant system with the greatest axial and torsional construct stiffness represents also the implant with the highest number of cycles until failure, and the other implants tested do not differ under cyclic loading. However, these results must be considered with caution because our singular mode of failure was plastic deformation of the plate (except one LCP). This will not represent the only mode of failure in the clinical situation.

Construct stiffness of a BIC is influenced by multiple factors. Not only does the choice of implants such as nails, conventional plates, or locking plates for the same fracture pattern alter construct stiffness [11, 19, 20], but also using locking plate fixation and different screw configurations such as using far cortical locking screws can alter the stiffness up to 81% [3]. Therefore, although using locking plate systems for distal femur fixation, the knowledge of basic differences in biomechanical performance configurations might help the surgeon in implant selection and/or altering his screw configuration. We evaluated four recent-generation implant systems for distal femur fixation to explore possible differences with a direct comparison. We found considerable differences in construct stiffness and fatigue, which may be attributable to implant design and implant material. Although the clinical transferability is always limited with experimental biomechanical experiments, knowledge of these differences may prove helpful in the clinical decision of which implant to choose or how to cope with difficult healing situations.

Acknowledgments We applied for consent of manufacturers of four available plate systems; consent was obtained from Stryker (Stryker GmbH, Selzach, Switzerland), Synthes (Synthes, Bettlach, Switzerland), Smith & Nephew (Smith & Nephew Inc, Memphis, TN, USA), and DePuy (DePuy International Ltd, Leeds, UK).

References

1. Augat P, Burger J, Schorlemmer S, Henke T, Peraus M, Claes L. Shear movement at the fracture site delays healing in a diaphyseal fracture model. *J Orthop Res.* 2003;21:1011–1017.
2. Augat P, Simon U, Liedert A, Claes L. Mechanics and mechano-biology of fracture healing in normal and osteoporotic bone. *Osteoporos Int.* 2005;16(Suppl 2):S36–43.
3. Bottlang M, Doomink J, Lujan TJ, Fitzpatrick DC, Marsh JL, Augat P, von Rechenberg B, Lesser M, Madey SM. Effects of construct stiffness on healing of fractures stabilized with locking plates. *J Bone Joint Surg Am*. 2010;92(Suppl 2):12–22.
4. Bottlang M, Lesser M, Koerber J, Doornink J, von Rechenberg B, Augat P, Fitzpatrick DC, Madey SM, Marsh JL. Far cortical locking can improve healing of fractures stabilized with locking plates. *J Bone Joint Surg Am.* 2010;92:1652–1660.
5. Doornink J, Fitzpatrick DC, Madey SM, Bottlang M. Far cortical locking enables fixation with periarticular locking plates. *J Orthop Trauma*. 2011;25:S29–34.
6. Duda GN, Schneider E, Chao EY. Internal forces and moments in the femur during walking. *J Biomech*. 1997;30:933–941.
7. Gaebler C, Speitling A, Milne EL, Stanzl-Tschegg S, Vécsei V, Latta LL. A new modular testing system for biomechanical evaluation of tibial intramedullary fixation devices. *Injury.* 2001;32:708–712.
8. Haidukewych G, Sems SA, Huebner D, Horwitz D, Levy B. Results of polyaxial locked-plate fixation of periarticular fractures of the knee. *J Bone Joint Surg Am.* 2007;89:614–620.
9. Henderson CE, Lujan T, Bottlang M, Fitzpatrick DC, Madey SM, Marsh JL. Stabilization of distal femur fractures with intramedullary nails and locking plates: differences in callus formation. *Iowa Orthop J*. 2010;30:61–68.
10. Henderson CE, Lujan TJ, Kuhl LL, Bottlang M, Fitzpatrick DC, Marsh JL. 2010 Mid-America Orthopaedic Association Physician in training award: healing complications are common after locked plating for distal femur fractures. *Clin Orthop Relat Res.* 2011; 469:1757–1765.
11. Higgins TF, Pittman G, Hines J, Bachus KN. Biomechanical analysis of distal femur fracture fixation: fixed-angle screw-plate construct versus condylar blade plate. *J Orthop Trauma.* 2007; 21:4–6.
12. Kregor PJ, Stannard JA, Zlowodski M, Cole PA. Treatment of distal femur fractures using the less invasive stabilization system: surgical experience and clinical results in 103 fractures. *J Orthop Trauma*. 2004;18:509–520.
13. Lujan TJ, Henderson CE, Madey SM, Fitzpatrick DC, Marsh JL, Bottlang M. Locked plating of distal femur fractures leads to inconsistent and asymmetric callus formation. *J Orthop Trauma.* 2010;24:156–162.
14. Marti A, Fankhauser C, Frenk A, Cordey J, Gasser B. Biomechanical evaluation of the less invasive stabilization system for the internal fixation of distal femur fractures. *J Orthop Trauma.* 2001;15:482–487.
15. Mueller ME, Nazarian S, Koch P, Schatzker J. *The Comprehensive Classification of Fractures of Long Bones.* Berlin, Germany: Springer Verlag; 1990:120–121.
16. Otto RJ, Moed BR, Bledsoe JG. Biomechanical comparison of polyaxial-type locking plates and fixed-angle locking plates for internal fixation of distal femur fractures. *J Orthop Trauma.* 2009;23:645–652.
17. Taylor SJG, Walker PS. Forces and moments telemetered from two distal femoral replacements during various activities. *J Biomech.* 2001;34:839–848.
18. Taylor SJG, Walker PS, Perry JS, Cannon SR, Woledge R. The forces in the distal femur and the knee during walking and other activities measured by telemetry. *J Arthroplasty.* 1998;13: 428–437.
19. Wähnert D, Hoffmeier K, Froeber R, Hofmann GO, Mueckley T. Distal femur fractures of the elderly—different treatment options in a biomechanical comparison. *Injury.* 2011;42:655–659.
20. Wähnert D, Hoffmeier KL, von Oldenburg G, Froeber R, Hofmann GO, Mueckley T. Internal fixation of type-C distal femoral fractures in osteoporotic bone. *J Bone Joint Surg Am*. 2010;92: 1442–1452.
21. Weckbach S, Losacco JT, Hahnhaussen J, Gebhard F, Stahel PF. Challenging the dogma on inferiority of stainless steel implants for fracture fixation. An end of the controversy? *Unfallchirurg.* 2012;115:79–79.
22. Weight M, Collinge C. Early results of the less invasive stabilization system for mechanically unstable fractures of the distal femur (AO/OTA types A2, A3, C2 and C3). *J Orthop Trauma.* 2004;18:503–508.
23. Wilkens KJ, Curtiss S, Lee MA. Polyaxial locking plate fixation in distal femur fractures: a biomechanical comparison. *J Orthop Trauma.* 2008,22:624–628.
24. Zlowodzki M, Williams S, Zardiackas LD, Kregor PJ. Biomechanical evaluation of the less invasive stabilization system and the 95 degree angled blade plate for the internal fixation of distal femur fractures in human cadaveric bones with high mineral density. *J Trauma.* 2006;60:836–840.
25. Zlodowski M, Williamson S, Cole PA, Zardiackas LD, Kregor PJ. Biomechanical evaluation of the less invasive stabilisation system, angled blade plate, and retrograde intramedullary nail for the internal fixation of distal femur fractures. *J Orthop Trauma.* 2004;18:494–502.